Possible Mitigation of Global Cooling due to Supervolcanic Eruption via Intentional Release of Fluorinated Gases

Yangyang Xu[1], Nathanael Philip Ribar[2], Gunnar W Schade[2], Andrew John Lockley[3], Yi Ge Zhang[2], Jeffrey Sachnik[2], Pengfei Yu[4], Jianxin Hu[5], and Guus J.M. Velders[6]

[1]TAMU
[2]Texas A&M University
[3]Andrew Lockley
[4]Institute for Environmental and Climate Research, Jinan University
[5]Peking University
[6]RIVM

May 13, 2023

Abstract

Supervolcanic eruptions induced abrupt global cooling (roughly at a rate of ˜1ºC/year lasting for years to decades), such as the prehistoric Yellowstone eruption released, by some estimates, SO2 about 100 times higher than the 1991 Mt. Pinatubo eruption. An abrupt global cooling of several ºC, even if only lasting a few years, would present immediate and drastic stress on biodiversity and food production - posing a global catastrophic risk to human society. Using a simple climate model, this paper discusses the possibility of counteracting supervolcanic cooling with the intentional release of greenhouse gases. Although well-known longer-lived compounds such as CO2 and CH4 are found to be unsuitable for this purpose, select fluorinated gases (F-gases), either individually or in combinations, may be released at gigaton scale to offset most of the supervolcanic cooling. We identify candidate F-gases (viz. C4F6 and CH3F) and derive radiative and chemical properties of 'ideal' compounds matching specific cooling events. Geophysical constraints on manufacturing and stockpiling due to mineral availability are considered alongside technical and economic implications based on present-day market assumptions. The consequences of F-gas release in perturbing atmospheric chemistry are discussed in the context of those due to the supervolcanic eruption itself. The conceptual analysis here suggests the possibility of mitigating certain global catastrophic risks via intentional intervention.

Hosted file

`962908_0_art_file_10965934_rt9v8q.docx` available at https://authorea.com/users/540715/articles/642445-possible-mitigation-of-global-cooling-due-to-supervolcanic-eruption-via-intentional-release-of-fluorinated-gases

1

Possible Mitigation of Global Cooling due to Supervolcanic Eruption via Intentional Release of

Fluorinated Gases

4

Yangyang Xu[1], Nathanael P. Ribar[1], Gunnar Schade[1], Andrew Lockley[2], Yi Ge Zhang[3],

Jeffrey T. Sachnik[1], Pengfei Yu[4], Jianxin Hu[5], Guus J. M. Velders[6,7]

7

8

[1]Department of Atmospheric Sciences, Texas A&M University, College Station, Texas, 77843,

USA,

[2]Bartlett School, University College London, United Kingdom,

[3]Department of Oceanography, Texas A&M University, College Station, Texas, 77843, USA,

[4]Jinan University, Guangzhou, Guangdong, China,

[5]Peking University, Beijing, China,

[6]National Institute for Public Health and the Environment (RIVM), Netherlands,

[7]Institute for Marine and Atmospheric Research Utrecht (IMAU), Utrecht University,

Netherlands

18

19

Corresponding author: Yangyang Xu (yangyang.xu@tamu.edu)

21

May 2023

23

Key Points:

- Several fluorinated greenhouse gases can reduce the magnitude of supervolcanic cooling to within natural variability.

- Radiative, physical and chemical properties of a hypothetical ideal compound can be estimated to mitigate specific volcanic cooling.

- Technical, economic and geophysical constraints and atmospheric chemistry consequences are discussed.

32   **Abstract**

33

34   Supervolcanic eruptions induced abrupt global cooling (roughly at a rate of ~1ºC/year lasting for

35   years to decades), such as the prehistoric Yellowstone eruption released, by some estimates, SO_2

36   about 100 times higher than the 1991 Mt. Pinatubo eruption. An abrupt global cooling of several

37   ºC, even if only lasting a few years, would present immediate and drastic stress on biodiversity

38   and food production - posing a global catastrophic risk to human society. Using a simple climate

39   model, this paper discusses the possibility of counteracting supervolcanic cooling with the

40   intentional release of greenhouse gases (GHGs). Although well-known longer-lived compounds

41   such as CO_2 and CH_4 are found to be unsuitable for this purpose, select fluorinated gases (F-

42   gases), either individually or in combinations, may be released at gigaton scale to offset most of

43   the supervolcanic cooling. We identify candidate F-gases (viz. C_4F_6 and CH_3F) and derive

44   radiative and chemical properties of 'ideal' compounds matching specific cooling events.

45   Geophysical constraints on manufacturing and stockpiling due to mineral availability are

46   considered alongside technical and economic implications based on present-day market

47   assumptions. The consequences of F-gas release in perturbing atmospheric chemistry are

48   discussed in the context of those due to the supervolcanic eruption itself. The conceptual analysis

49   here suggests the possibility of mitigating certain global catastrophic risks via intentional

50   intervention.

51

52

1 Introduction

While the world is grappling with global warming, some have called attention to the risk of a much more abrupt global cooling due to natural or human causes (e.g., Robock et al., 2009; Coupe et al., 2019). At least three drivers of global cooling are global catastrophic risks (Bostrom and Cirkovic, 2008): thermonuclear warfare (Mills et al., 2014; Coupe et al., 2019), asteroid impacts (Vellekoop et al., 2014; Bardeen et al., 2017), and supervolcanic eruptions (Timmreck & Graf, 2005; Robock et al., 2009; Fendley et al., 2019; Black et al., 2021; Cassidy & Mani, 2022). All involve injections of absorbing and/or reflective materials into the upper atmosphere, reducing tropospheric and surface solar radiation flux. Consequently, global average surface temperatures would drastically decline over just a few years, gradually recovering as the injected materials deposit back to the surface.

For nuclear detonations, black carbon (soot) from urban firestorms is lofted into the stratosphere via efficient shortwave (SW) absorption and subsequent thermal transfer to and convection of the surrounding air mass (Coupe et al., 2019). Large asteroid impacts inject soot due to global forest firestorms and potentially also due to SO_2 released from vaporized crust near the point of impact. Ocean cooling following the bolide impact at the Cretaceous - Paleogene boundary (~66 Mya) was up to 7°C along the Gulf coast (Vellekoop et al., 2014). The degree of cooling and the relative significance of cooling agents depend on factors such as the impact location and angle as well as the explosive power (Toon et al., 1997).

For supervolcanic eruptions, sulfur dioxide (SO_2) is released from crust/mantle rock at high temperatures. Intense heat within the volcanic plume results in convection into the stratosphere (Robock et al., 2009; Timmreck, 2012). In the stratosphere, SO_2 takes weeks to

form sulfate aerosols, which scatter SW radiation back to space, leading to surface cooling. For example, the 1815 Mt. Tambora eruption on the island of Sumbawa, Indonesia (Self et al., 1984) led to the subsequent "year without a summer" (1816). Such planetary scale events possess great destructive power and the potential to generate a global cooling at a rate of 1 ºC/year (Robock et al., 2009), which is about 100 times faster than contemporary global warming (on average less than 0.01 ºC/year since the industrial revolution). In comparison, CO_2 outgassing from volcanic eruptions contributed to paleoclimatic warming on a much longer timescale of centuries to millennia and only led to an even smaller warming rate (Black et al., 2018).

Though temperature recovery after such events could be on the order of a decade, ecosystems and human society would face major and potentially irreversible disruption. Agricultural yields, highly sensitive to changes in surface climate and solar insolation, would plunge worldwide (Scherrer et al., 2020; Da et al., 2021), likely resulting in the collapse of supply chains, subsequent civil disorder, and regional conflicts (Wilcox et al., 2015). It is, therefore, worth investigating preparation for potential mitigation.

Could global cooling events even be mitigated? Current thoughts mainly concern prevention. Concerns over a nuclear winter scenario were a catalyst for the 1980's arms treaties between the USA and the Soviet Union, but recent nuclear proliferation has caused renewed worries over regional wars (Coupe et al., 2019; Mills et al., 2014; Toon et al., 2014, Toon et al., 2019). Defense against asteroid impacts via early detection and kinetic redirection has been investigated (e.g., NASA's DART program), though recent studies suggest various extents of efficacy (Cheng et al., 2018; El Mir et al., 2018). By contrast, preparation for volcanic eruptions is primarily adaptive, with monitoring implemented to provide an early warning (potentially years ahead) for evacuation (Morton, 2021). Additionally, some engineering proposals to cool

subterranean magma chambers have been suggested (Wilcox et al., 2015; Denkenberger and Blair, 2018). However, such strategies may have the potential to induce phase changes within the chamber, enhancing hydrothermal explosions (Wilcox et al., 2015).

Anthropogenic warming, while associated with catastrophic risks itself, has inspired investigation into intentional climate intervention (geoengineering), such as Solar Radiation Management, which aims to lower global temperatures through space mirror deployment (e.g., Teller et al., 1997; 2002) or stratospheric aerosol injection (SAI; National Academy of Science, 2018) - which mimics volcanic cooling. "Counter-geoengineering" has also been discussed, considering injections of greenhouse gases (GHGs) to counteract SAI (Parker et al., 2018). The research question we consider here is: could deliberate releases of GHGs reduce the magnitude of supervolcanic cooling without subsequently producing undesirable consequences?

To address this question, global cooling due to a hypothetical supervolcanic 2 Gt SO_2 injection is simulated by a simple climate model here. This amount is similar in scale to the injection from the Yellowstone eruption (Timmreck and Graf, 2005) or a lower bound estimate of the Toba eruption (Robock et al., 2009), both of which were estimated to have a similar SO_2 injection rate and a Volcanic Explosivity Index (VEI) of 8. Our research extends Fuglestvedt et al. (2014), which used a global climate model to simulate the role of chlorofluorocarbons in offsetting the cooling due to the smaller Tambora eruption (with a VEI of 7; Newhall et al., 2018) by instead directly modeling a large suite of commercially available F-gases to identify potential offsetting candidates. Additionally, a brief discussion is offered on the geophysical, technical, and economic constraints on the production as well as the potential side effects on atmospheric chemistry. We do not recommend real-world preparations for deployment be taken soon; but instead, we intend to motivate further study and discussion regarding the proactive

122   mitigation of such global catastrophic risks, particularly those due to anthropogenic or natural

123   climate changes.

124

125   **2 Methods**

126

127   2.1 Energy balance climate model

128   We utilize a zero-dimension energy balance model. This is inspired by Hasselman (1976)

129   and was recently used by Ramanathan and Xu (2010), Xu and Ramanathan (2017), and Hanna et

130   al. (2021). With the evolution of mass emission over a certain time interval as the desired model

131   input, atmospheric concentration, top-of-atmosphere (TOA) forcing (Wm^{-2}), and surface

132   temperature response (°C) are estimated.

133   For methane, CH$_4$, mass emission is used to derive concentration ($C(t)$; unit: parts per

134   billion [ppb]) with the following equation (Eqn. 1).

135

$$C(t) = 715 + \left(\sum_{i=0}^{t} \frac{E[i]}{2.78} * e^{\frac{-(t-i-1)}{\tau}} \right) - \left(715 * \left(1 - e^{\frac{-t}{\tau}} \right) \right) \qquad (1)$$

137   In Eqn. 1, E and t are the mass emission and time (in years) for a given year i, and τ is the e-

138   folding lifetime of CH$_4$ (12 years per the Intergovernmental Panel on Climate Change [IPCC]

139   Assessment Report 5 [AR5], assumed to be constant in this analysis). The conversion factor from

140   the emission of 1 Mt to the atmospheric concentration of 1 ppb is 2.78 (ppb/Mt) (Table 7.6 in

141   IPCC AR4 Working Group I [WGI]). We assumed a preindustrial concentration (to avoid

142   considering the complexity of contemporary climate change) of 715 ppb (IPCC AR5) and natural

143   emissions of 100 Mt per year.

144   The direct forcing of CH_4 has a square root relationship with concentration ($F_D(t)$ in

145   Eqn. 2, ignoring the overlapping effect with N_2O since it is not modeled here), resulting in a

146   marginally smaller response to concentration. The indirect forcings due to atmospheric

147   chemistry, such as stratospheric water vapor (0.07 Wm^{-2}), formation of CO_2 (0.016 Wm^{-2}), and

148   tropospheric ozone (0.2 Wm^{-2}), are smaller in magnitude. Thus, they are simply scaled here from

149   the CH_4 concentration linearly (Eqn. 3-5, for stratospheric water vapor, CO_2, and tropospheric

150   ozone, respectively). The coefficients are obtained from IPCC AR5 WGI, Chapter 8, as their

151   separate contribution to the present-day (2005) forcing relative to the preindustrial (1850). The

152   total forcing for CH_4 (F; unit: Wm^{-2}), on an annual basis (t), is then calculated in Eqn. 6.

153

154     $$F_D(t) = 0.57 * \left(\frac{\sqrt{C(t)} - \sqrt{C_{1850}}}{\sqrt{C_{2005}} - \sqrt{C_{1850}}} \right) \tag{2}$$

155     $$F_{I1}(t) = 0.07 * \left(\frac{C(t) - C_{1850}}{C_{2005} - C_{1850}} \right) \tag{3}$$

156     $$F_{I2}(t) = 0.016 * \left(\frac{C(t) - C_{1850}}{C_{2005} - C_{1850}} \right) \tag{4}$$

157     $$F_{I3}(t) = 0.2 * \left(\frac{C(t) - C_{1850}}{C_{2005} - C_{1850}} \right) \tag{5}$$

158     $$F(t) = F_D + F_{I1} + F_{I2} + F_{I3} \tag{6}$$

159

160   For the F-bearing compounds, the concentration can be estimated from the time-varying

161   emission and molar mass:

162

163     $$C(t) = C(t-1) + (E(t) \times \alpha) - C(t-1) \times (1 - e^{-\frac{1}{\tau}}) \tag{7}$$

164

165   In Eqn. 7, E(t) is the emission amount at a given time step (in kt), and α is a mass

166   conversion factor. The default time step is a day, considering their short lifetime of 0.5 to 3

167   years. Additional simulations using a longer time step of a month or a year were also tested for

168   the shorter-lived Compound B (see below), which produced a high bias in concentration due to

169   the omission of decay during the initial time step (the first month or the first year). The simulated

170   concentration and forcing using a time step of a day and a month largely converged (see further

171   discussion later). The conversion factor between mass emission and atmospheric concentration,

172   α, is the mixing ratio of 1 kt emission (10^9 gram divided by m, which is molar mass in g/mol)

173   with respect to the total molar count of the atmosphere. The final concentration is expressed in

174   the unit of ppb, hence the multiplier of 10^9:

175

176    $$\alpha = \frac{\left(\frac{1e9\,g}{m}\right)}{\left(\frac{5e21\,g}{28.97\,g/mol}\right)} \times 1e9 \tag{8}$$

177

178   The conversion to radiative forcing from the concentration is based on the radiative

179   efficiency ($Wm^{-2}\ ppb^{-1}$) of the agents provided in Hodnerog et al. (2020). Some saturation in

180   absorption bands could occur such that the linear relation could no longer be valid. If so, the

181   GHG radiative forcing contribution will continue to increase, albeit at a lower rate. In that case,

182   the necessary F-gas emissions estimated here will be biased low. However, the magnitude of this

183   bias is difficult to quantify due to the lack of quantitative information in the literature.

184   In all cases (volcanic-related emissions, CH_4, and F-gases), we regard the forcing

185   numbers as the instantaneous forcing at the TOA without considering the fast adjustment of

186   clouds and stratosphere (effective radiative forcing). The total forcing generated by all

187   compounds will collectively drive the temperature response using the following equation:

188

$$T(t) = T[0] + \sum_0^{i_t} \left(\frac{1\ year}{C_p \times \rho \times z} \times \left(F[i] - \frac{T[i]}{s} \right) \right)$$ (9)

190

191   where T and F are the temperature and forcing for a given year; C_p and ρ are the specific

192   heat and density of seawater; z is the depth of the effective ocean mixed layer; s is climate

193   sensitivity expressed in the unit of °C/(Wm^{-2}). The time step in Eqn. 9 is adopted to be one year.

194   We tested the sensitivity to the time step assumption in Ramanathan et al. (2022) (one year vs.

195   one month) in the context of global climate mitigation in the next few decades, and the results

196   using different time steps were consistent. We do not directly implement the shorter (daily or

197   monthly) time steps in the forcing-temperature response function of Eqn. 9 for three reasons.

198   First, the radiative forcing formulation (concentration and forcing for CH$_4$ and F-gas) is based on

199   empirical approximation at an annual mean (and global average) basis after accounting for the

200   seasonal dependence of the background thermal radiation from the Earth that would affect the

201   radiative efficiency. Second, the literature does not provide a supervolcanic forcing time series in

202   the necessary daily or monthly resolution. Third, the emission rate of F-gas is estimated to match

203   the annual mean supervolcanic forcing. Therefore, any bias in quantifying temperature response

204   using the energy balance equation would operate equally in both the warming and cooling case

205   and does not directly affect the emission estimates.

206   Regardless, as a robustness check, we implement the shorter time step (daily or monthly)

207   in the emission-concentration relationship (Eqn. 7) in one case. After obtaining the concentration

208   at the daily or monthly resolution, we convert it to an annual mean with a running average before

209   quantifying its radiative forcing (using the formulations constructed on an annual mean basis)

210   and temperature response (using Eqn. 9 at the annual time step). This is presented in Figure 6.

211

2.2 Validation of the climate model

The 1991 eruption of Mt. Pinatubo injected ~20 Mt SO_2, the effects of which have been closely observed and extensively studied (Stenchikov et al., 1998; Ramachandran et al., 2000; Soden et al., 2002). Observations from Pinatubo are used to test model fidelity (Figure 1), specifically the conversion of eruption-driven radiative flux anomalies into global average temperature response.

Using observed monthly mean SW and longwave (LW) flux anomalies (covering only 60°S-60°N), the annual average of total TOA (top of atmosphere) forcing is calculated and input into the model (Figure 1a). The effective ocean mixed layer depth (z in Eqn. 9) is assumed to be relatively small (35 m) to reflect the short temporal scale of the Pinatubo eruption and the limited role of oceanic thermal inertia. The simulated cooling largely agrees with the observed global average temperature drop of approximately 0.4 °C at Year 2, with a recovery curve also aligning closely with published data (Figure 1b) (Soden et al., 2002; Bender et al., 2010).

The model was also used to simulate the temperature response to a 2 Gt SO2 emission scenario with a prescribed forcing (Figure 2a; Robock et al., 2009). While the prescribed forcing in Robock et al. (2009) might be an overestimate according to other studies (Timmreck et al., 2010; Lane et al., 2013; Smith et al., 2018; Black et al., 2018), this model also tracks Robock et al.'s published temperature response well, which was derived using a more complex global climate model. Here we used a configuration of z=50 m and s=0.45 °C/(Wm^{-2}) for the five years post-eruption (Figure 2b). The effective ocean mixed layer depth (z) of 50 m is a reasonable assumption given the short duration of the forcing, and agrees with Fuglestvedt et al. (2014) who adopted a slab ocean model with a fixed depth of 54 m. The smaller climate sensitivity of 0.45

234 °C/Wm^{-2} is used, presumably because some positive climate feedback, such as ice-related

235 surface albedo feedback, is not fully involved at a short timescale of 1-5 years.

236   The lack of a second (deeper) ocean box neglects the increasing role of the ocean in

237 buffering the forcing and thus makes the recovery too quick compared to Robock et al.'s coupled

238 climate model. Our recent works (Ramanathan et al., 2022; Chen et al., 2021; Chen et al., 2020)

239 used a two-box energy balance model with a coupled carbon cycle. Since CO_2 emission is not

240 directly relevant to this paper, we use the simpler 1-box model over the 2-box configuration.

241 This 1-box model has also been used and validated extensively (Dreyfus et al., 2022; Xu and

242 Ramanathan, 2017; Xu et al., 2013). Previous careful comparisons with the two-box version and

243 the more complex MAGICC model have been made (Hanna et al., 2021). Therefore, the utility

244 and limitations of the 1-box model are well documented and justify its application here.

245   To fully demonstrate model sensitivity to the role of ocean heat content in buffering the

246 response to forcing, Figure 2b shows temperature response assuming a larger effective ocean

247 layer depth (80 meters) after Year 5, which produces a better fit to the coupled ocean-atmosphere

248 global climate model results. Similar to the concern of time step issues addressed in Section 6.2d,

249 the assumption of effective ocean mixed layer depth (z) does not directly affect the derivation of

250 required F-gas emission since the F-gas warming will also be prolonged by the same fraction

251 with a larger z and a close match with the volcanic radiative forcing will be maintained.

252

253 2.4 OH decay rate perturbation due to fluorinated gases (F-gases)

254   The enhanced decay rate of OH (in s^{-1}) due to a specific F-gas is estimated using

255 $(d[OH]/dt)/[OH] = - k(F\text{-}gas)*[F\text{-}gas]$, where [OH] and [F-gas] is the molecular density (number

256 of molecules per cm^3) and k(F-gas) is the reaction rate constant in cm^3/molecules/s. k(F-gas) is

257 estimated by 1/(lifetime*[OH]) without considering temperature dependence, where the average

258 global [OH] is $\sim 10^6$ molecules/cm^3 (Brasseur et al., 1999). [F-gas] is calculated from the mixing

259 ratio multiplied by atmospheric molecular density ($\sim 2.5*10^{19}$ molecules/cm^3). The background

260 OH decay rate, primarily due to atmospheric CO and CH_4, is similarly estimated, based on [CO]

261 and [CH_4] as well as k(CO) and k(CH_4) (Brasseur et al., 1999).

262

263 **3. Results**

264

265 3.1 Simulated cooling in response to supervolcanic eruption

266   A supervolcanic cooling event (e.g., with a VEI of 8) has not been observed in recent

267 history, so any associated analysis must rely on mass flux approximations. Robock et al. (2009)

268 presented a range of estimates for the Toba eruption 74,000 years ago, highlighting 6 Gt SO_2

269 (300x Pinatubo) as "most likely". This study considers the lower estimate of 2 Gt (100x

270 Pinatubo) in Robock et al. (2009), close to assumptions in Timmreck and Graf (2005) for

271 Yellowstone. Recent work has uncovered two previously unknown supereruptions from

272 Yellowstone, the largest of which (Grey's Landing, 8.7 Ma BP) is 11% larger than the second-

273 largest (Huckleberry Ridge, 2.1 Ma BP) (Knott et al., 2020; Timmreck and Graf, 2005). Thus,

274 the mass emissions for supervolcanic eruptions such as Yellowstone and Toba are highly

275 uncertain, and a determination of the actual magnitude is beyond the scope of this work.

276   Since our energy balance model cannot resolve the troposphere and stratosphere, forcing

277 estimates from previous 3D modeling are used (Robock et al., 2009). A large 50 Wm^{-2} TOA

278 forcing (Figure 2a) is converted from the surface SW forcing time series presented in Figure 4 of

279 Robock et al. (2009). The conversion is needed because of the offset of the LW warming effect

280   of volcanic aerosols and stratospheric solar absorption. The conversion factor of 0.5

281   (Net_TOA/SW_surface) is estimated from the numbers in Figure 5 by Timmreck et al. (2005)

282   and Table 2 by Timmreck et al. (2012), suggesting a ratio of 0.4 to 0.6. Volcanic particulate

283   matter, CO_2, and H_2O emissions have been neglected here. CO_2 emissions, even from large

284   volcanic eruptions, have small impacts on the timescale of years to decades (Timmreck et al.,

285   2012; Ramachandran et al., 2000).

286   In response to a Yellowstone-like 2 Gt SO_2 injection, fossil records show a high survival

287   rate of African megafauna and Indian hominids, implying more limited cooling than previously

288   predicted (Timmreck et al., 2012). Modeling with detailed microphysical processes of formation

289   and growth of sulfate aerosols (Timmreck et al., 2010; Timmreck et al., 2012) suggests a third of

290   the cooling assumed by Robock et al. (2009). Forcing estimates in Robock et al. (2009), as

291   adopted here, are thus considered likely overestimates due to omitting sulfate aerosol size

292   distribution dependence (Timmrick et al., 2012). Nevertheless, our main purpose is to determine

293   whether the concept of F-gas injection is generally feasible rather than targeting any particular

294   cooling scenario. Forthcoming studies may address more realistic scenarios, including the

295   uncertainty of forcing magnitude and temporal sequences.

296   Figure 2b shows a simulated plunge in the global annual average temperature of more

297   than 10 °C following a 2 Gt SO_2 injection into the upper atmosphere. The cooling decreases after

298   three years, and the temperature gradually recovers to within 1°C of the initial climate state

299   approximately a decade after the eruption - emulating 3-D global climate model outputs (dashed

300   line in Figure 2b). Temperatures rebound as coagulation and fallout of stratospheric sulfate

301   aerosol occurs. Given its magnitude, the comparatively short cooling period can still be globally

302   disastrous, e.g., due to net primary productivity decline. Cooling could be prolonged if volcanic

303 eruptions cluster over a long or even geologic period, with continental flood basalt events (e.g.,

304 Siberian and Deccan Traps) being extreme examples (Sayyed, 2013).

305   The discrepancy between this model and Robock's global climate model estimates as the

306 temperature recovers (Figure 2b, after Year 6) is possibly due to fixing effective ocean mixed

307 layer depth (z) as a constant throughout our simulation rather than allowing it to increase (as

308 inherently in global climate models where a deeper ocean would carry more heat inertia and

309 therefore make the recovery from the imposed forcing slower). This model sensitivity is

310 demonstrated in Figure 2b (see Methods Section). This model limitation, while not directly

311 affecting the main results in the later section on the required magnitude of F-gas emissions, will

312 need to be improved in future analyses, especially when considering the forcing sequence (e.g.,

313 multiple subsequent eruptions).

314   To fully comprehend the large forcing and cooling rate here, we first consider the

315 possibility of directly releasing natural gas. Its main constituent, CH_4, has a GWP100 of 28

316 (global warming potential over 100 year time scale being 28 times larger than CO2) and a

317 GWP20 of 84 (IPCC AR5). Figure 3a shows this scenario; the required mass release of CH_4 is

318 very large (200 Gt vs. current natural gas production of ~2.9 Gt/year (3.8 trillion cubic meters;

319 IEA, 2021). Figure 3a shows that injected CH_4 cannot avoid "overshoot" as the initial success in

320 offsetting the supervolcanic cooling (despite an unrealistically high emission requirement) is

321 followed by an overheating of more than 5 ºC for many years, which would also be disastrous.

322 The decadal lifetime of CH_4 is too long to counter abrupt but temporary cooling. Moreover, the

323 actual CH_4 lifetime under such a large release would be even longer due to an associated

324 reduction of atmospheric OH levels in response to the CH_4 injection (the primary CH_4 sink).

325   Matching the required response time of the forcing and the lifetime of warming agents is

326   central to the selection of candidate gases. As a model sensitivity exercise, the CH_4 lifetime was

327   lowered to 2 years. Radiative efficiency was simultaneously increased by 35 times to 0.027 Wm^{-2}

328   ^{2}ppb^{-1}, testing if the required mass release can be lowered correspondingly. The simulated

329   temperature response obtained is encouraging. The temperature response curve of this "unstable

330   and short-lived" designer compound (Figure 3b) is opposite to the supervolcanic cooling with

331   comparable magnitude and achieved at a much lower emission rate of 6 to 3.5 Gt in Years 1 and

332   2. This exercise prompted an examination of other existing short-lived compounds with higher

333   radiative efficiency.

334

335   3.2 Temperature responses to F-gas injections

336   Fluorinated gases (F-gases) have been known contributors to global warming since the

337   latter half of the 20th century, with radiative forcing equivalent to 18% of CO_2, despite

338   concentrations at least six orders of magnitude smaller (Hodnerog et al., 2020). These

339   compounds are widely used as refrigerants, fire suppression agents, and for blowing foam

340   insulation (Velders et al., 2015). Most are non-toxic, non-flammable, and non-reactive., Other F-

341   gases – especially HFCs – have increased in production after the agreement of the Montreal

342   Protocol in 1987, which phased out the use of ozone-depleting Cl- and Br-bearing F-gases

343   (CFCs, HCFCs, Bromocarbons) (Velders et al., 2009). The increased use of HFCs is also a target

344   of climate mitigation for the 21st century (Xu et al., 2013; Velders et al., 2015; UNEP & IEA,

345   2020).

346   HFCs have a wide range of atmospheric lifetimes (from months to 40 years) and global

347   warming potentials (GWP100 ranging from <1 to 4,790) (Hodnerog et al., 2020). Analysis of

348   CH_4 (Section 2) suggests shorter lifetimes and higher radiative efficiencies are needed. Thus, in

349   our selections, we deliberately exclude compounds with lifetimes longer than 3.5 years to

350   mitigate the issue of persistent overheating. Excluding compounds with lifetimes below 0.5 years

351   (reactive halogens, typically ranging from days to weeks) avoids the requirement for near-

352   continuous releases. Ozone-depleting Br- and Cl-bearing gases and those containing oxygen

353   atoms (due to their more complex structures) were also excluded from the analysis. Table 1 lists

354   the resulting potential candidates selected from the 5-page-long Table 5 in Hodnerog et al.

355   (2020).

356   The candidates in Table 1 were further narrowed by selecting those with a higher

357   GWP100/lifetime ratio (rightmost column). GWP100/lifetime was used as the ranking criterion

358   over GWP100 for multiple reasons. First, GWP100 represents integrated forcing (akin to

359   temperature response) over 100 years. Second, GWP100/lifetime is sensitive to both radiative

360   efficiency and lifetime, as opposed to only radiative efficiency. And third, GWP100 alone does

361   not closely correlate with near-term warming (a few years after emission), the focus of this

362   study. Assuming the same radiative efficiency and molar weight, the same instantaneous mass

363   release will last longer in the atmosphere with a longer lifetime and will produce larger warming

364   over 100 years (hence a larger GWP100).

365   The release of the top five compounds was modeled separately. The model was run

366   numerous times for each compound, with the magnitude and timing of emissions adjusted after

367   each run to approach a minimized temperature residual - defined as within a +/- 1 °C range of the

368   pre-eruption level throughout the entire post-eruption recovery (Figure 4a-e). We discuss the

369   properties of these five identified compounds below, ordered by GWP100/lifetime ratio (Table

370   1).

371   Compound A, C_4HF_5 (Pentafluoro-cyclobutene in Figure 4a), has a lifetime of 0.7 years;

372   and a GWP100 of 97. Emission deployment after optimization is 6.0 Gt in Year 1 and 6.5 Gt in

373   Years 2-3 (Figure 5a), distributed evenly over 365 days of a year. The response residual after

374   mitigation is in the range of -1.4 to 0.9 °C (Figure 5b). Its lowest GWP (among the five

375   compounds tested here) and shortest lifetime necessitate a greater amount of total emissions to

376   offset the specific cooling.

377   Compound B, C_4F_6 (Hexafluoro-cyclobutene in Figure 4b), has a lifetime of 1 year and a

378   GWP100 of 132. In order to offset the cooling, it requires an emission deployment of 8.25 Gt in

379   the Year 1 post-eruption, followed by 2.75 Gt in Years 2-3 (Figure 5a). This is a promising

380   candidate, offsetting the cooling almost entirely, with the residual falling within a 1ºC level

381   (Figure 5b).

382   Compound C, CH_3CHF_2 (HFC-152a in Figure 4c), has a lifetime of 1.6 years and

383   GWP100 of 172. The optimized emission sequence is 5.6 Gt in Year 1 and 5.5 Gt in Year 2.

384   Similar to C_4F_6, HFC-152a can greatly offset cooling with a slightly less massive emission,

385   maintaining a residual below ±1 °C.

386   Compound D, $CH_2FCHFCF_3$ (HFC-245eb in Figure 4d), has a lifetime of 3.2 years and a

387   GWP100 of 341. It only needs a single-year release of 6.75 Gt in Year 1 alone. The longer

388   lifetime and larger GWP enable the least amount of total mass release. However, the temperature

389   response residual is less ideal (in contrast to A with the shortest lifetime) and can be as large as

390   1.3 to 2.6°C.

391   Compound E, CH_3F (HFC-41 in Figure 4e), has a lifetime of 2.8 years and GWP100 of

392   142. This compound requires the largest release rate (16 Gt in Year 1, 1.5 Gt in Year 2) due to its

393   low radiative efficiency (an order of magnitude smaller than Compound D of HFC-245eb, Table

394   1). This deficiency is offset by a longer lifetime, hence the relatively large GWP. Although the

395   temperature residual is one of the least ideal among other compounds, its chemical simplicity

396   may imply smaller production costs and environmental effects (see Sections 4 and 5).

397   Compounds with lifetimes below 2 years (A, B, C) and higher GWP/lifetime ratios offer

398   more satisfactory emission sequences and temperature residuals (Figures 4 and 5). Moreover,

399   C_4F_6 and HFC-152a both reduce the eruption-induced cooling to within a 1°C range for the

400   entire duration of the experiment period. In contrast, the lower GWP/lifetime ratios in D and E

401   produce undesirable cooling and warming due to excessive lifetime. This is especially apparent

402   for HFC-245eb in Figure 4d, despite it having the highest GWP of the tested compounds.

403   Additionally, the metric of integrated radiative forcing can be used to interpret the

404   temperature response to diverse compounds (Figure 6). Radiative forcing (Figure 6b) and

405   integrated radiative forcing (Figure 6c) are shown for two representative F-gases with similar

406   GWP (to contrast with the volcanic forcing also plotted in Figures 6b and c). Total mass releases

407   of HFC-41 and C_4F_6 are 14 Gt and 8.3 Gt, respectively, despite having similar GWP (142; 132).

408   The resulting volume concentrations are different by roughly an order of magnitude (Figure 6a)

409   due to HFC-41's much smaller molar weight. However, both instantaneous and integrated

410   radiative forcings are similar, given C_4F_6's larger radiative efficiency (Table 1).

411   Clearly, the integrated radiative forcing in Figure 6c can approximate the temperature

412   counterbalance well for short-lived gases. The difference in temporal response is also consistent

413   with the temperature simulation in Figure 4. For example, HFC-41 (red) shows an initial

414   underheating followed by an overheating (Figure 6c). C_4F_6 maintains a closer mirroring of

415   integrated forcing with respect to volcanic eruptions (Figure 6c, blue)—also shown in the match

416   of temperature trajectories up to Year 4, after which an under-compensation is found.

417   While these five shortlisted compounds show promise in mitigating most of the cooling,

418   they are designed and manufactured for different purposes and are clearly not ideal. We lastly

419   discuss the possibility of a designer compound (Figure 4f) that can be tuned to produce almost

420   exactly the desired cooling mitigation (residual <0.5 ºC) – statistically indistinguishable from

421   interannual climate variability. As an exploratory exercise, this 'ideal' compound is speculated to

422   possess the largest radiative efficiency of 0.3 $Wm^{-2}ppb^{-1}$ found in C_4F_6 (Figure 4b), while

423   maintaining a small molar weight of 67 similar to HFC-152a (Figure 4c). Fine-tuning the mass

424   emission sequences to achieve the right amount of warming (Year 1-4 at 2.75 Gt, 2.25 Gt, 0.75

425   Gt, and 0.5 Gt, respectively; the rightmost bar in Figure 5a) suggests a lifetime of ~0.9 years —

426   between that of C_4HF_5 (Figure 4a) and C_4F_6 (Figure 4b). While we refrain from making

427   recommendations on the elemental composition and molar structure, the identified characteristics

428   (molar weight, radiative efficiency, and lifetime) above are similar to those existing, suggesting

429   the possibility of designing an 'ideal' compound mixture.

430

431   **4 Discussion**

432

433   4.1 Geophysical, technical, and economic limitations

434   Fluorine used to manufacture F-gases is extracted from mined fluorspar (CaF_2) and

435   fluorapatite ($Ca_5(PO_4)_3F$) ores. Post-extraction, these minerals are directly refined (fluorspar) or

436   chemically converted (fluorapatite) into pure CaF_2, the primary material in the production of F-

437   bearing gases (Jaccaud, 2020). There is an estimated 5 Gt of CaF_2 equivalent extractable reserve

438   on the Earth (USGS, 2020), about 2.5 Gt of F-equivalent. Based on our calculation, HFC-245eb

439   requires the least amount of elemental fluorine (70% of its total mass), about 4.2 Gt in total (all

440   needed in Year 1). Yet, this elemental fluorine mass is still at least three orders of magnitude

441   larger than the present-day production of about 7 million tons annually (Hayes et al., 2017).

442   The required production would consume nearly all of the currently estimated global CaF_2

443   reserves, but mineable reserves may increase with future exploration. This constraint may be

444   alleviated by tapping into the ocean-based source. Approaches to extracting dissolved F ions

445   from the ocean exist (Tressaud, 2008), but a close examination of technical details and costs is

446   beyond the scope of this paper. The fluorine content of seawater ranges between 1 and 1.4 mg/L

447   (Jaccaud et al., 2020). Presuming a mineable shallow (300 m) surface ocean with a volume of

448   roughly 100 million km^3, up to 150 Gt of fluorine could be extracted, far more than the required

449   F mass of the single-digit Gt scale.

450   Jaccaud et al. (2020) placed the price of elemental fluorine (F, molar weight = 19 g/mol)

451   at \$5-8 per kilogram, based on extracting from mineral sources only, not the ocean. As a rough

452   estimate, adopting the value of \$5 per kilogram (presuming future economies of scale) and

453   doubling this cost for incorporation into the HFC, manufacturing the compound with the smallest

454   F requirement out of the five compounds tested (HFC-245eb), 4.8 Gt during deployment, would

455   cost a total of 48 trillion dollars, twice the modern US GDP — an exercise justifiable as an

456   alternative to global calamity.

457   Considering the lead time for scaling up production capacity, studies have shown that

458   extreme magnitude eruptions are likely preceded by some geologic signals (Wilson et al., 2021),

459   providing possible predictability. However, given the limited monitoring capacity and unknown

460   factors contributing to eruptive timing and magnitude, the range of lead times is wide - from

461   days to decades (Wilson et al., 2021; Morton, 2021). In an optimistic scenario with ample lead

462   time, F-gas stockpiles could be, in principle, manufactured in advance. Such an enormous

463 accumulation of F-gas would be an inarguably complex project, accompanied by similarly

464 complex economic, engineering, and security concerns. A thorough cost-benefit analysis would

465 require in-depth collaboration between climatologists and experts in these fields, which is

466 beyond this proof-of-concept study.

467   This analysis identified properties of a single candidate; however, a cocktail of novel

468 "designer" compounds (fluorinated or not)—with enhanced absorption efficiency, mixed

469 lifetimes, and reasonable production cost—could be developed and manufactured. Similar

470 proposals exist in the context of geoengineering (Cao et al., 2017) and counter-geoengineering

471 (Parker et al., 2018). Future, detailed analyses to assess such strategies' technological and

472 economic feasibility are anticipated.

473

474 4.2 Chemical consequences

475   Gigaton-scale releases of compounds containing C-H bonds, coupled with a marked

476 decline in solar radiation reaching the troposphere, could also disrupt the tropospheric chemistry

477 of the hydroxyl radical (OH). A large depletion of tropospheric OH as a major chemical sink,

478 especially in the boundary layer near surface release points, could exacerbate air pollution issues

479 due to primary emissions of CO and VOCs by increasing their lifetimes. The OH loss rate due to

480 F-gases can be calculated and compared to the loss rate due to background CH_4 and CO

481 abundance at ~ 1 s^{-1} (Methods; Brasseur et al., 1999). Our model estimates approximately a 100

482 to 150 ppb initial abundance of C_4F_6 after release and instantaneous dilution (Figure 6a) –

483 equivalent to a 0.1 to 0.15 s^{-1} OH reactivity. This is equivalent to a 10-15% drop from the

484 background, which can significantly increase CH_4 lifetime. Reductions in OH due to F-gas

485 oxidation followed by an increase in the lifetime of background CH_4 would induce additional

486   warming, implying less F-gas is needed. In the case of CH_3F (HFC-41), our calculation (Figure

487   6a) shows that the average tropospheric mixing ratio would be as high as 2000 ppb, which could

488   create an OH loss rate of ~0.6 s^{-1}, more disruptive than C_4F_6. However, even assuming the 60%

489   drop in OH decay rate and subsequent CH_4 lifetime increase, this would only lead to a rough

490   doubling of CH_4 concentration from the background level. Following Eqn. 6, this translates to

491   about an increase of 0.5 Wm^{-2}, almost two orders of magnitude smaller than the direct forcing

492   from F-gases (Figure 6b).

493   Chemical interactions between F-gas releases and volcanic SO_2 emissions could lead to

494   secondary effects on atmospheric chemistry. F-gases may alter SO_2 and sulfate lifetimes, with

495   consequences for cooling and recovery timeline. The oxidation of released F-gas could lead to

496   slower SO_2 oxidation (due to lower OH levels) to form sulfate aerosols and thus mute the

497   volcanic cooling response, similar to the competing effects of a large volcanic eruption itself

498   leading to slower SO_2 oxidation (Stevenson et al., 2003). Dynamically, the tropospheric warming

499   due to F-gases may alter the circulation pattern that changes the lifetime of stratospheric

500   aerosols. These complex chemical and dynamic interactions are not yet included in the simple

501   climate modeling analysis reported herein.

502   Other adverse environmental and health impacts could result from first or second-order

503   F-gas reaction products, which may be toxic. FHCO, the first reaction product of CH_3F, may

504   accumulate near release sites; its aqueous formation of HF could have health and environmental

505   effects due to gas-phase exposure or acid rain. Due to these ecological risks, the impact needs to

506   be mitigated by monitoring and facilitating the mineralization of fluorine upon degradation from

507   the injected gases. Adverse perturbations to biogeochemical cycling need to be placed in the

508   context of the supervolcanic eruption, which would have already significantly disrupted the

509   stratospheric ozone layer and tropospheric chemistry, followed by acid rain and tropospheric

510   haze due to aerosol fallout.

511

512   4.3 Limitation on spatially balanced temperature response

513   Despite successfully rebalancing global mean temperature using F-gas releases, a

514   mismatch in spatial distribution is likely (Fuglestvedt et al., 2014); relative underheating is found

515   in the tropics, where aerosol-induced cooling is stronger than at higher latitudes (Fuglestvedt et

516   al., 2014). Vertically, some overheating is possible in the stratosphere, where volcanic aerosols

517   lead to strong local heating, warming of the tropopause, and disruption of typical stratospheric

518   dynamics. These spatial mismatches are also known issues for SAI, and potential fixes have been

519   proposed via a strategic release in a specific latitude, altitude, and season (Tilmes et al., 2017;

520   Tilmes et al., 2018; Visioni et al., 2019; Xu et al., 2020). A similar strategy with multi-location

521   (varying different latitudes) surface release could be employed with F-gases, given their

522   similarly short lifetimes. More complex modeling strategies must be used to test these

523   possibilities, such as energy balance models with higher dimensions (North & Kim, 2017) or a

524   global climate model (Fuglestvedt et al., 2014).

525   Fuglestvedt et al. (2014) used a global climate model with a spatial resolution of

526   1.9°x2.5°, providing valuable insights into regional and hydrological impacts; however, it was

527   not suited for screening candidate compounds due to computational resource constraints. This

528   analysis also advances beyond Fuglestvedt et al. (2014), because the previous study only

529   considered a much smaller eruption (3x the magnitude of the 1991 Pinatubo eruption) and a

530   single hypothetical compound (with radiative properties equivalent to CFC-11 but a shorter

531 lifetime and no impact on stratospheric ozone) and it only discussed side effects such as

532 stockpile leakage very briefly (see their p. 14).

533

534 **5. Conclusion**

535

536 Super volcanic eruptions can lead to abrupt global cooling for years to a decade. The

537 disruption to food production and social systems would be enormous and is considered a

538 potential global catastrophic risk. This modeling study analyzed the possibility of releasing

539 selected greenhouse gases to offset global cooling due to volcanic aerosols. We examined a suite

540 of commercially available F-gases with varying radiative efficiency and lifetime and identified a

541 few leading candidates for such an undertaking (Table 1). Specifically, we examined the suite of

542 F-gases in Hodnerog et al. (2020) with lifetimes between 0.5 and 3.5 years to avoid the issues of

543 persistent overheating and continuous deployment. Br and Cl-bearing gases were excluded due

544 to ozone depletion, as well as those containing oxygen due to their more complex structure.

545 Selected gases would need to be manufactured, stocked, and released at Gt-scale to

546 counterbalance a Yellowstone-like super volcanic eruption. We found that even after such a

547 large-scale eruption, the residual temperature changes could be kept within typical year-to-year

548 natural variability. The desired physical and chemical properties of an 'ideal compound' were

549 identified, which would almost completely offset the known cooling when released in

550 subsequent years after the eruption. The actual selection of a compound to combat a super

551 volcanic eruption and the necessary mass release of this compound is dependent on the specific

552 volcanic cooling. Longer-lived greenhouse gases such as methane are clearly not fit for purpose

553 due to the short-term nature of volcanic cooling.

554   While 'ideal' compounds (or their combinations) with Gt-scale release appear to be

555   capable of offsetting the volcanic cooling, detailed discussions on the limitations and caveats of

556   this approach are offered. These include the production limitations due to the geophysical

557   constraints on mineral availability, as well as the technical and economic constraints (estimated

558   based on the current market). While it is possible that future technology development can relax

559   some of these constraints, the environmental consequences of massive F-gas release, both on the

560   perturbation to the atmospheric oxidation capacity and precipitation acidification, and also on the

561   spatial pattern of temperature responses need further scrutiny. However, these side effects may

562   be tolerable in comparison to the immense consequences of unmitigated cooling.

563   The analysis presented here suggests global catastrophic risks due to abrupt cooling could

564   at least be partially mitigated with artificial approaches. Due to the prototypical nature of this

565   analysis, here we do not suggest real-world deployment in the near future. Producing massive

566   amounts of F-gas seems to be limited by land-based mineral availability, and further economic

567   analysis is hindered by the technical uncertainty in oceanic extraction. Moreover, due to the large

568   uncertainty of cooling magnitude, preemptive manufacturing and large-scale stockpiling are

569   needed. Still, no assessment is available on technical solutions for transport and storage, as well

570   as associated risks such as inadvertent leakage.

571   This study advances the necessary discussion regarding the proactive mitigation of global

572   catastrophic risks and aims to inspire more research in this direction. Similar concepts were

573   presented in the literature, at least qualitatively, such as releasing GHGs or heating aerosols as

574   counter-measures in response to unilateral solar-radiation geoengineering (Parker et al., 2018) or

575   injecting substances that bind to sulfate aerosols to reduce their atmospheric lifetime in response

576   to supervolcanic eruptions (Cassidy and Mani, 2022). Others considered volcanic eruption

577   prevention via direct cooling of subterranean magma chambers (Wilcox et al., 2015;

578   Denkenberger and Blair, 2018). To safeguard the long-term continuity of human civilization,

579   such forward-thinking should not be restricted (which is unfortunately argued for in Biermann et

580   al. 2022).

581

Open Research

All underlying data needed to understand, evaluate, and build upon the reported research, as well as the Python code for the modeling and data analysis, will be openly shared upon acceptance and publication.

596

597

References

599

Archer, David, et al. "Atmospheric Lifetime of Fossil Fuel Carbon Dioxide." *Annual Review of Earth and Planetary Sciences*, vol. 37, no. 1, 2009, pp. 117–134., https://doi.org/10.1146/annurev.earth.031208.100206.

Bardeen, Charles G., et al. "On Transient Climate Change at the Cretaceous−Paleogene Boundary Due to Atmospheric Soot Injections." *Proceedings of the National Academy of Sciences*, vol. 114, no. 36, 2017, https://doi.org/10.1073/pnas.1708980114.

Biermann, Frank, et al. "Solar Geoengineering: The Case for an International Non-Use Agreement." *WIREs Climate Change*, 17 Jan. 2022, 10.1002/wcc.754. Accessed 21 Jan. 2022.

Black, Benjamin A., et al. "Global Climate Disruption and Regional Climate Shelters after the Toba Supereruption." *Proceedings of the National Academy of Sciences*, vol. 118, no. 29, 2021, https://doi.org/10.1073/pnas.2013046118.

Black, Benjamin A., et al. "Systemic Swings in End-Permian Climate from Siberian Traps Carbon and Sulfur Outgassing." *Nature Geoscience*, vol. 11, no. 12, 2018, pp. 949–954., https://doi.org/10.1038/s41561-018-0261-y.

Brasseur, Orlando, and Tyndall. Atmospheric Chemistry and Global Change, Oxford University Press, 1999.

618   Bostrom, Nick, and Milan M. Cirkovic. *Global Catastrophic Risks*. Oxford University

619   Press, 2008.

620   Cao, Long, et al. "Simultaneous Stabilization of Global Temperature and Precipitation

621   through Cocktail Geoengineering." Geophysical Research Letters, vol. 44, no. 14,

622   2017, pp. 7429–7437., https://doi.org/10.1002/2017gl074281.

623   Cassidy, M., & Mani, L. (2022). Huge volcanic eruptions: time to prepare. In Nature

624   (Vol. 608, Issue 7923, pp. 469–471). Springer Science and Business Media LLC.

625   https://doi.org/10.1038/d41586-022-02177-x

626   Chen J., H. Cui, Y. Xu and Q. Ge (2021) Long-term temperature and sea-level rise

627   stabilization before and beyond 2100: Estimating the additional climate mitigation

628   contribution from China's recent 2060 carbon neutrality pledge. Environ. Res.

629   Lett. 16 074032

630   Chen, J., Cui, H., Xu, Y. & Ge, Q. An Investigation of Parameter Sensitivity of Minimum

631   Complexity Earth Simulator. Atmosphere. 11(1), (2020).

632   Cheng, Andrew F., et al. "AIDA DART Asteroid Deflection Test: Planetary Defense and

633   Science Objectives." *Planetary and Space Science*, vol. 157, 2018, pp. 104–115.,

634   https://doi.org/10.1016/j.pss.2018.02.015.

635   Coupe, Joshua, et al. "Nuclear Winter Responses to Nuclear War Between the United

636   States and Russia in the Whole Atmosphere Community Climate Model Version

637   4 and the Goddard Institute for Space Studies ModelE." *Journal of Geophysical*

638   *Research: Atmospheres*, vol. 124, no. 15, 2019, pp. 8522–8543.,

639   https://doi.org/10.1029/2019jd030509.

Da, Y., Xu, Y. & McCarl, B. Effects of Surface Ozone and Climate on Historical (1980–2015) Crop Yields in the United States: Implication for Mid-21st Century Projection. Environmental and Resource Economics (2021). https://doi.org/10.1007/s10640-021-00629-y.

Denkenberger, David C., and Robert W. Blair. "Interventions That May Prevent or Mollify Supervolcanic Eruptions." *Futures*, vol. 102, 2018, pp. 51–62., https://doi.org/10.1016/j.futures.2018.01.002.

Dreyfus, G. B., Xu, Y., Shindell, D. T., Zaelke, D., & Ramanathan, V. (2022). Mitigating climate disruption in time: A self-consistent approach for avoiding both near-term and long-term global warming. Proceedings of the National Academy of Sciences, 119(22), e2123536119.

Fendley, Isabel M., et al. "Constraints on the Volume and Rate of Deccan Traps Flood Basalt Eruptions Using a Combination of High-Resolution Terrestrial Mercury Records and Geochemical Box Models." *Earth and Planetary Science Letters*, vol. 524, 2019, p. 115721., https://doi.org/10.1016/j.epsl.2019.115721.

Fuglestvedt, J. S., B. H. Samset, and K. P. Shine (2014), Counteracting the climate effects of volcanic eruptions using short-lived greenhouse gases, Geophys. Res. Lett., 41, 8627–8635, doi:10.1002/2014GL061886.

Ganopolski, A., Winkelmann, R. & Schellnhuber, H. Critical insolation–CO2 relation for diagnosing past and future glacial inception. Nature 529, 200–203 (2016). https://doi.org/10.1038/nature16494

Hanna, Ryan, et al. "Emergency Deployment of Direct Air Capture as a Response to the Climate Crisis." *Nature Communications*, vol. 12, no. 1, 2021, https://doi.org/10.1038/s41467-020-20437-0.

Hasselmann, K. "Stochastic Climate Models Part I. Theory." *Tellus*, vol. 28, no. 6, 1976, pp. 473–485., https://doi.org/10.3402/tellusa.v28i6.11316.

Hayes, T.S., et al., Critical mineral resources of the United States—Economic and environmental geology and prospects for future supply: U.S. Geological Survey Professional Paper 1802, p. G1–G80, 2017, http://doi.org/10.3133/pp1802G.

Hodnebrog, Ø., et al. "Updated Global Warming Potentials and Radiative Efficiencies of Halocarbons and Other Weak Atmospheric Absorbers." *Reviews of Geophysics*, vol. 58, no. 3, 2020, https://doi.org/10.1029/2019rg000691.

IEA (2021), Natural Gas Information: Overview, IEA, Paris https://www.iea.org/reports/natural-gas-information-overview

IPCC, 2014: Climate Change 2014: Synthesis Report. Contribution of Working Groups I, II and III to the Fifth Assessment Report of the Intergovernmental Panel on Climate Change [Core Writing Team, R.K. Pachauri and L.A. Meyer (Eds.)]. IPCC, Geneva, Switzerland, 151 Pp.

Jaccaud, Michel, et al. "Fluorine." *Ullmanns Encyclopedia of Industrial Chemistry*, 2020, pp. 1–19., https://doi.org/10.1002/14356007.a11_293.pub2.

Knott, T.R., et al., 2020, Discovery of two new super-eruptions from the Yellowstone hotspot track (USA): Is the Yellowstone hotspot waning?: *Geology*, v. 48, p. 934–938, https://doi.org/10.1130/G47384.1

683   Li, Mengze, et al. "Tropospheric OH and Stratospheric OH and Cl Concentrations
684   Determined from CH4, CH3Cl, and SF6 Measurements." *Npj Climate and*
685   *Atmospheric Science*, vol. 1, no. 1, 2018, https://doi.org/10.1038/s41612-018-
686   0041-9.

687   U.S. Geological Survey, 2020, Mineral commodity summaries 2020: U.S. Geological
688   Survey, pp. 60-61., https://doi.org/10.3133/mcs2020.

689   Mills, Michael J., et al. "Multidecadal Global Cooling and Unprecedented Ozone Loss
690   Following a Regional Nuclear Conflict." *Earth's Future*, vol. 2, no. 4, 2014, pp.
691   161–176., https://doi.org/10.1002/2013ef000205.

692   Mir, Charles El, et al. "A New Hybrid Framework for Simulating Hypervelocity Asteroid
693   Impacts and Gravitational Reaccumulation." *Icarus*, vol. 321, 2019, pp. 1013–
694   1025., https://doi.org/10.1016/j.icarus.2018.12.032.

695   Morton, Mary Caperton. "Don't Call It a Supervolcano." *Eos*, 28 Sept. 2021,
696   https://eos.org/features/dont-call-it-a-supervolcano.

697   National Academies of Sciences, Engineering, and Medicine. 2021. *Reflecting Sunlight:*
698   *Recommendations for Solar Geoengineering Research and Research Governance*.
699   Washington, DC: The National Academies Press.https://doi.org/10.17226/25762.

700   Newhall et al., 2018: Anticipating future Volcanic Explosivity Index (VEI) 7 eruptions
701   and their chilling impacts. Geosphere, 14, No. 2, 1-32, doi:10.1130/GES01513.1

702   The Nobel Committee for Physics. "Scientific Background on the Nobel Prize in Physics
703   2021: For Groundbreaking Contributions to Our Understanding of Complex
704   Physical Systems." The Royal Swedish Academy of Sciences, 2021.

Parker, A., et al. "Stopping Solar Geoengineering through Technical Means: A Preliminary Assessment of Counter-Geoengineering." Earth's Future, vol. 6, no. 8, 2018, pp. 1058–1065., https://doi.org/10.1029/2018ef000864.

Robock, Alan, et al. "Did the Toba Volcanic Eruption of ~74 Ka B.P. Produce Widespread Glaciation?" *Journal of Geophysical Research*, vol. 114, no. D10, 2009, https://doi.org/10.1029/2008jd011652.

Ramachandran, S., et al. "Radiative Impact of the Mount Pinatubo Volcanic Eruption: Lower Stratospheric Response." *Journal of Geophysical Research: Atmospheres*, vol. 105, no. D19, 2000, pp. 24409–24429., https://doi.org/10.1029/2000jd900355.

Ramanathan, V., Xu, Y. & Versaci, A. Modelling human–natural systems interactions with implications for twenty-first-century warming. Nat Sustain (2021). https://doi.org/10.1038/s41893-021-00826-z

Sayyed, M.r.g. "Flood Basalt Hosted Palaeosols: Potential Palaeoclimatic Indicators of Global Climate Change." *Geoscience Frontiers*, vol. 5, no. 6, 2014, pp. 791–799., https://doi.org/10.1016/j.gsf.2013.08.005.

Scherrer, Kim J. N., et al. "Marine Wild-Capture Fisheries after Nuclear War." *Proceedings of the National Academy of Sciences*, vol. 117, no. 47, 2020, pp. 29748–29758., https://doi.org/10.1073/pnas.2008256117.

Self, S., Rampino, M.R., Newton, M.S., Wolff, J.A., 1984. Volcanological study of the great Tambora eruption of 1815. Geology, 12, 659 – 663.

Soden, Brian J., et al. "Global Cooling After the Eruption of Mount Pinatubo: A Test of Climate Feedback by Water Vapor." *Science*, vol. 296, no. 5568, 2002, pp. 727–730., https://doi.org/10.1126/science.296.5568.727.

Stenchikov, Georgiy L., et al. "Radiative Forcing from the 1991 Mount Pinatubo Volcanic Eruption." *Journal of Geophysical Research: Atmospheres*, vol. 103, no. D12, 1998, pp. 13837–13857., https://doi.org/10.1029/98jd00693.

Stevenson, D. S., Johnson, C. E., Highwood, E. J., Gauci, V., Collins, W. J., and Derwent, R. G.: "Atmospheric impact of the 1783–1784 Laki eruption: Part I Chemistry modeling", Atmos. Chem. Phys., 3, 487–507, https://doi.org/10.5194/acp-3-487-2003, 2003.

Teller, Edward, Lowell Wood, Hoover Institution, and Roderick Hyde. "Global Warming and Ice Ages:" In The Carbon Dioxide Dilemma, 22. UCRL-JC 135414. Livermore, California: Lawrence Livermore National Laboratory, 1997.

Teller, Edward, Roderick Hyde, and Lowell Wood. "Active Climate Stabilization: Practical Physics-Based Approaches to Prevention of Climate Change." Livermore, California: Lawrence Livermore National Laboratory, 2002.

Tilmes, Simone, et al. "Sensitivity of Aerosol Distribution and Climate Response to Stratospheric SO2 Injection Locations." *Journal of Geophysical Research: Atmospheres*, vol. 122, no. 23, 2017, https://doi.org/10.1002/2017jd026888.

Tilmes, Simone, et al. "CESM1(WACCM) Stratospheric Aerosol Geoengineering Large Ensemble Project." *Bulletin of the American Meteorological Society*, vol. 99, no. 11, 2018, pp. 2361–2371., https://doi.org/10.1175/bams-d-17-0267.1.

Timmreck, Claudia, et al. "Aerosol Size Confines Climate Response to Volcanic Super-Eruptions." *Geophysical Research Letters*, vol. 37, no. 24, 2010, https://doi.org/10.1029/2010gl045464.

Timmreck, Claudia, et al. "Climate Response to the Toba Super-Eruption: Regional Changes." *Quaternary International*, vol. 258, 2012, pp. 30–44., https://doi.org/10.1016/j.quaint.2011.10.008.

Timmreck, C. and Graf, H.-F.: The initial dispersal and radiative forcing of a Northern Hemisphere mid-latitude super volcano: a model study, Atmos. Chem. Phys., 6, 35–49, https://doi.org/10.5194/acp-6-35-2006, 2006

Toon, Owen B., et al. "Environmental Perturbations Caused by the Impacts of Asteroids and Comets." *Reviews of Geophysics*, vol. 35, no. 1, 1997, pp. 41–78., https://doi.org/10.1029/96rg03038.

Toon, Owen B., et al. "Environmental Consequences of Nuclear War." *AIP Conference Proceedings,* 2014, https://doi.org/10.1063/1.4876320.

Toon, Owen B., et al. "Rapidly Expanding Nuclear Arsenals in Pakistan and India Portend Regional and Global Catastrophe." *Science Advances*, vol. 5, no. 10, 2019, https://doi.org/10.1126/sciadv.aay5478.

United Nations Environment Programme and International Energy Agency (2020). Cooling Emissions and Policy Synthesis Report: Benefits of cooling efficiency and the Kigali Amendment. UNEP, Nairobi and IEA, Paris. (pdf, UNEP press release)

Velders, G. J. M., et al. "The Large Contribution of Projected HFC Emissions to Future Climate Forcing." Proceedings of the National Academy of Sciences, vol. 106, no. 27, 2009, pp. 10949–10954., https://doi.org/10.1073/pnas.0902817106.

Velders, Guus J.m., et al. "Future Atmospheric Abundances and Climate Forcings from Scenarios of Global and Regional Hydrofluorocarbon (HFC) Emissions." Atmospheric Environment, vol. 123, 2015, pp. 200–209., https://doi.org/10.1016/j.atmosenv.2015.10.071.

Vellekoop, J., et al. "Rapid Short-Term Cooling Following the Chicxulub Impact at the Cretaceous-Paleogene Boundary." *Proceedings of the National Academy of Sciences*, vol. 111, no. 21, 2014, pp. 7537–7541., https://doi.org/10.1073/pnas.1319253111.

Visioni, D., MacMartin, D. G., Kravitz, B., Tilmes, S., Mills, M. J., Richter, J. H., and Boudreau, M. P. (2019). "Seasonal Injection Strategies for Stratospheric Aerosol Geoengineering". *Geophysical Research Letters*, 1-10. https://doi.org/10.1029/2019GL083680

Wilcox, Brian. "Defending Human Civilization from Supervolcanic Eruptions." 2015, https://scienceandtechnology.jpl.nasa.gov/sites/default/files/documents/Defending CivilizationFromSupervolcanos20151015.pdf.

Wilson, Colin J. N., et al. "No Single Model for Supersized Eruptions and Their Magma Bodies." *Nature Reviews Earth & Environment*, vol. 2, no. 9, 2021, pp. 610–627., https://doi.org/10.1038/s43017-021-00191-7.

790   Xu, Y., et al. "The Role of HFCs in Mitigating 21st Century Climate Change."

791   *Atmospheric Chemistry and Physics*, vol. 13, no. 12, 2013, pp. 6083–6089.,

792   https://doi.org/10.5194/acp-13-6083-2013.

793   Xu, Y., et al. "Climate Engineering to Mitigate the Projected 21st-Century Terrestrial

794   Drying of the Americas: a Direct Comparison of Carbon Capture and Sulfur

795   Injection." *Earth System Dynamics*, vol. 11, no. 3, 2020, pp. 673–695.,

796   https://doi.org/10.5194/esd-11-673-2020.

797   Xu, Y., and V. Ramanathan (2017), Well below 2 °C: Mitigation strategies for avoiding

798   dangerous to catastrophic climate changes. Proc. Natl. Acad. Sci. ,

799   doi:10.1073/pnas.1618481114 .

Table 1. A list of F-gas candidates ranked by lifetimes (0.5 to 3.2 years). The five rows in boldface are compounds selected for further modeling analysis due to their higher GWP/lifetime ratio (A-E, ranked by this ratio [large to small]).

804

Chemical identifier	Formula (+ Molar weight)	Lifetime (yr)	Radiative Efficiency (Wm^{-2}ppb^{-1})	GWP100	ratio = GWP100 /lifetime
HFC-152	CH$_2$FCH$_2$F	0.5	0.05	23	46
1,3,3,4,4,5,5-heptafluoro cyclopentane	cyc (-CF$_2$CF$_2$CF$_2$CF=CH-)	*0.6*	*0.21*	47	78
1,3,3,4,4-pentafluorocyclob utene (A)	**cyc (-CH=CFCF$_2$CF$_2$-), (144 g/mol)**	**0.7**	***0.27***	**97**	**139**
Hexafluorocyclob utene (B)	**cyc (-CF=CFCF$_2$CF$_2$-), (162 g/mol)**	***1***	***0.3***	**132**	**132**
HFC-263fb	CH$_3$CH$_2$CF$_3$	1.1	*0.1*	78	71
Octafluorocyclopen tene	cyc (-CF$_2$CF$_2$CFCF$_2$CF$_2$-)	1.1	*0.25*	82	75
1,1,2,2,3,3-hexafluorocyclopen	cyc (-CF$_2$CF$_2$CF$_2$CH$_2$CH$_2$-)	*1.6*	*0.2*	126	79

tane					
HFC-152a (C)	**CH₃CHF₂ (66 g/mol)**	**1.6**	**0.1**	**172**	**108**
HFC-41 (E)	**CH₃F (34 g/mol)**	**2.8**	**0.02**	**142**	**50.7**
1,1,2,2,3,3,4-heptafluorocyclopentane	cyc (-CF₂CF₂CF₂CHFCH₂-)	2.8	0.24	243	86.8
HFC-245ea	CHF₂CHFCHF₂	3.2	0.16	267	83.4
HFC-245eb (D)	**CH₂FCHFCF₃ (**134 g/mol)	**3.2**	**0.2**	**341**	**106.6**
(4R,5R)-1,1,2,2,3,3,4,5-octafluorocyclopentane	trans-cyc (-CF₂CF₂CF₂CHFCHF-)	3.2	0.26	271	84.7

805
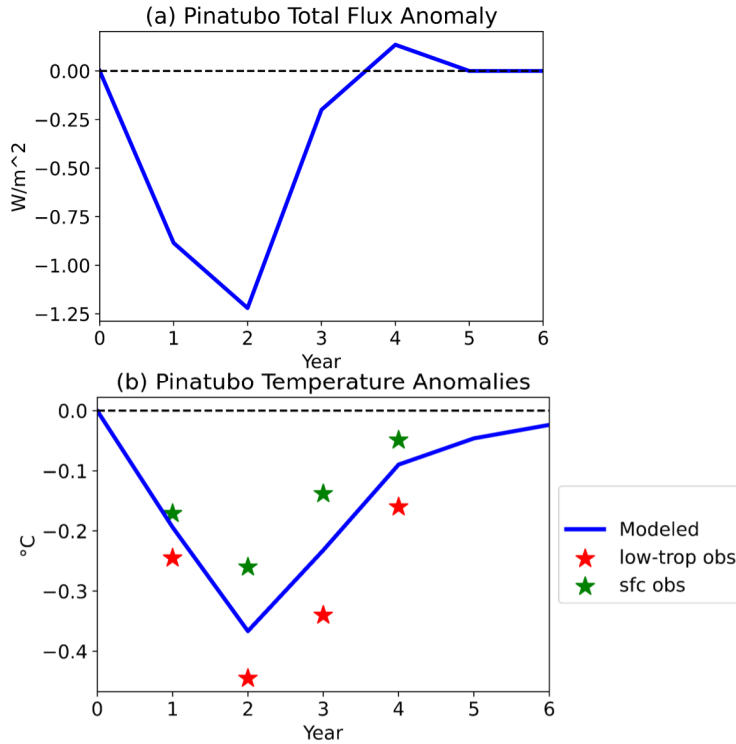
Figure 1. (a) TOA radiative flux anomaly following the Pinatubo eruption, calculated from shortwave and longwave monthly observations (Figure 1 in Soden et al., 2002). (b) Surface temperature response in our model, compared to the lower troposphere and surface observations (Soden et al., 2002; Bender et al., 2010). Year Zero on the x-axis represents June 1990 to May 1991, the year preceding the eruption in June 1991.
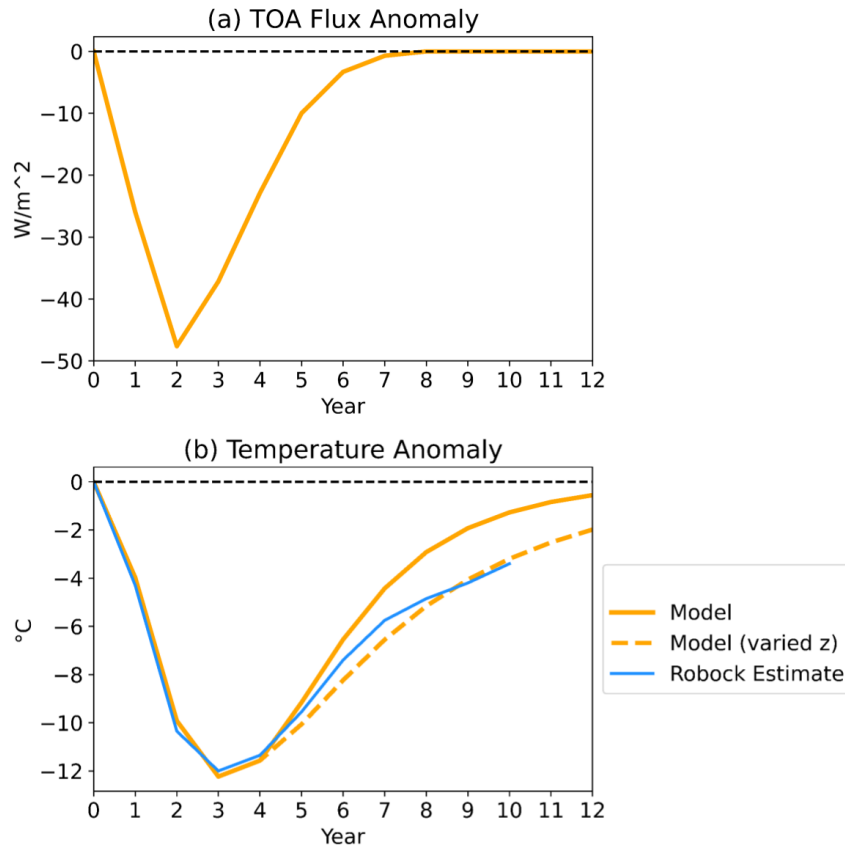
Figure 2. (a) TOA radiative forcing following a 2-Gt SO_2 injection (converted from the shortwave surface forcing estimates in Figure 4 of Robock et al., 2009). (b) Simulated global surface cooling (orange solid line) using the forcing estimates in (a), which is compared with Robock et al. (2009) (blue solid line). The orange dash line is also simulated by our model, but assuming the effective ocean depth (z) increases from 50 to 80 meters in Year 5.
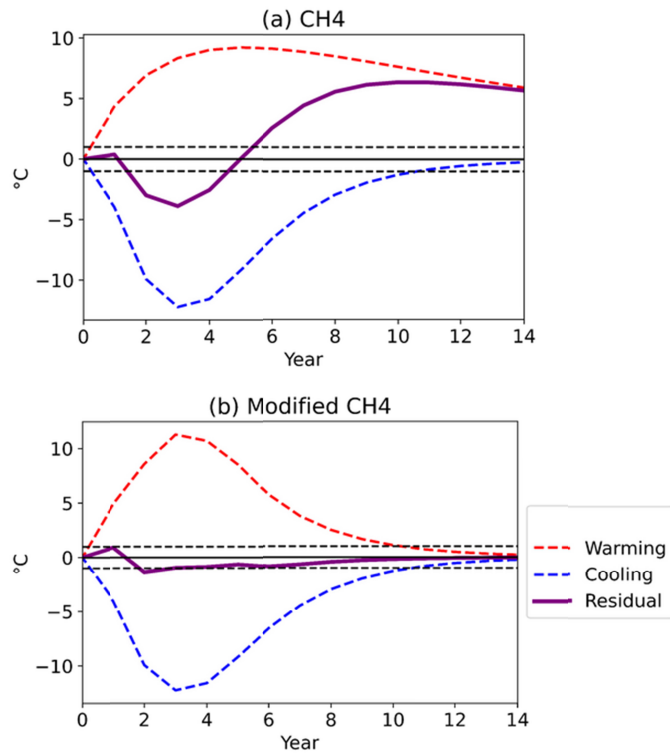
819

Figure 3. (a) Supervolcanic cooling mitigation via a hypothetical 200 Gt CH₄ emission in Year 1, which is clearly infeasible. The blue dashed line is cooling due to the volcanic eruption. The red dashed line is heating due to GHG release. The solid purple line represents the residual (i.e., summation of cooling and heating). Targeted [-1ºC, 1ºC] limits are shown as horizontal dashed lines. (b) Similar mitigation via a 6 Gt "CH₄"-like emission (with stronger radiative efficiency and shorter lifetime) in Year 1, followed by 3.5 Gt releases in Years 2 and 3.
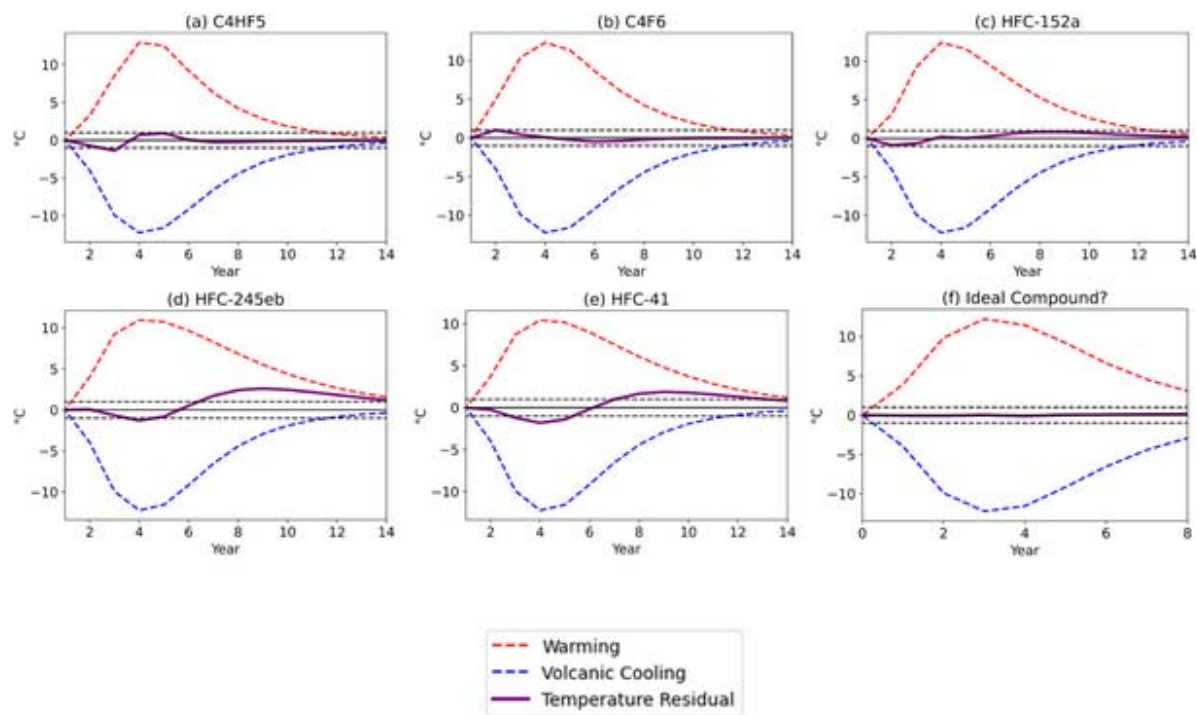
827

Figure 4. Simulated volcanic cooling and warming offset by F-gas emission. (a) C_4HF_5; (b) C_4F_6; (c) HFC-152a; (d) HFC-245eb; (e) HFC-41 (CH_3F); and (f) a possible compound with ideal characteristics. The blue dashed line is cooling due to volcanic eruption. The red dashed line is heating due to F-gases. Each purple solid line represents the residual (net temperature effect), which aims to fall mostly into the 1ºC range indicated by the horizontal dashed lines. Note that in (f) the timeline is shortened to Year 0 to 8 to demonstrate a clear optimal counterbalancing by the 'ideal' compound.
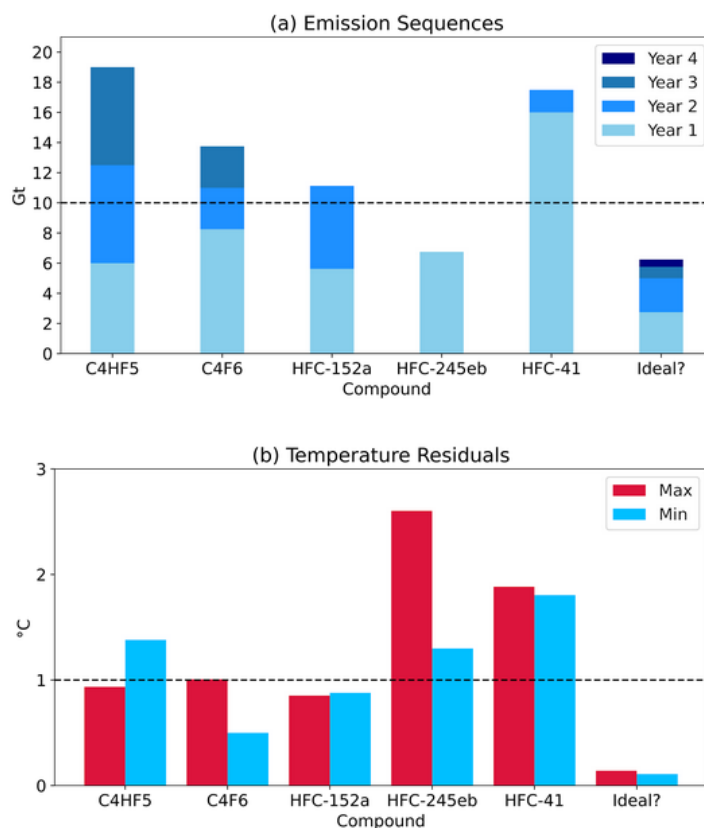
Figure 5. (a) The sequencing of annual emission of the five identified compounds, as well as the "ideal" compound. The sequence of emission is constructed via simple model runs with optimized results shown in Figure 4. (b) The range of temperature residuals as seen in Figure 4, which is targeted to be kept below 1ºC.
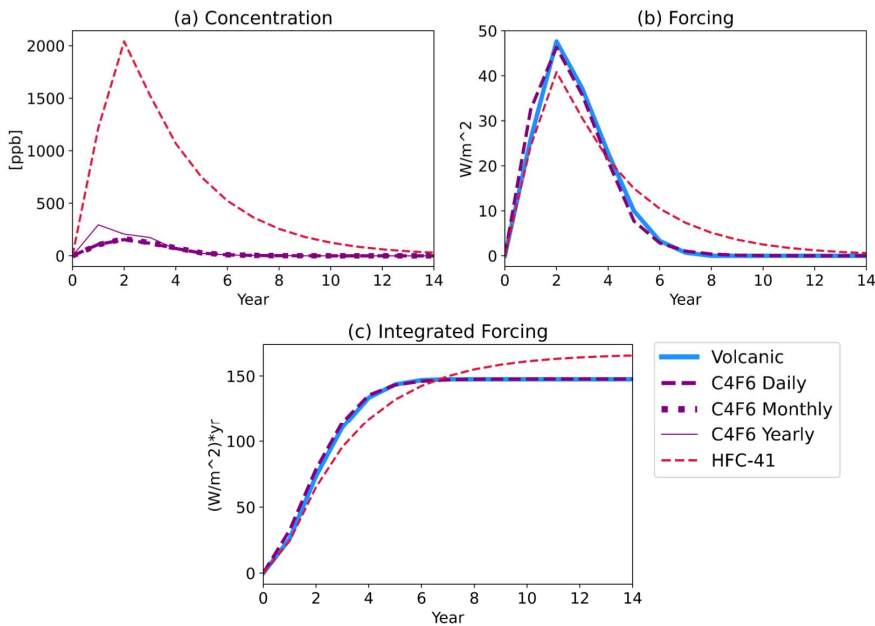
840

841

Figure 6.

(a) Simulated average atmospheric concentrations of C₄F₆ (Compound B, purple dashed line C₄F₆ daily) and HFC-41 (Compound E, red dashed line). Results using monthly (purple dot-dash line) and yearly (purple solid thin line) time steps, respectively, are also included as a robustness check for the shorter-lived C₄F₆. The monthly time steps show very good agreement with the default results using daily steps, while the yearly time steps produce a concentration biased high.

(b) and (c): simulated radiative forcing and integrated radiative forcing, respectively, of C₄F₆ (Compound B, purple dashed line C₄F₆ daily) and HFC-41 (Compound E, red dashed line). Volcanic forcing (blue solid line) as in Figure 2 is shown again for reference.

852

853

854